A Harmonically-Terminated Two-Gram Low-Power Rectenna on a Flexible Substrate

Sean Korhummel, Dr. Daniel G. Kuester, and Prof. Zoya Popović
Dept. of Electrical, Computer and Energy Engineering
University of Colorado
Boulder, Colorado 80309
Email: dkuester@colorado.edu, korhummel@colorado.edu, zoya@colorado.edu

***Abstract*—A 900 MHz low-cost flexible omni-directional rectenna with a mass of 2.1 grams is demonstrated. A rectenna as demonstrated here employs only a Schottky diode, a capacitor, and a printed coplanar circuit which presents class-F harmonic terminations to the diode, resulting in approximately 48.6% efficiency at a low 8 μW/cm^2 incident power density. The rectenna is printed on 0.13 mm PET with a commercial printing process depositing 1 µm-thick conductive traces.**

I. Introduction

Non-directive far-field powering where the available incident power densities are low, on the order of micro-watts per cm^2 [3], [2] has gained attention in recent years, especially for powering unattended wireless sensors [4], [3]. The power is radiated either from dedicated compliant low- power transmitter(s) which is in general narrowband, or harvested from already available sources, which can be broadband [5], [2]. Modulated transmission has also been investigated in [2] for multi-tone signals, and in [6] for chaotic waveforms. The position of the transmitters and receiving devices can vary and is not in general known precisely, requiring non-directional antennas and power reception circuits that can maintain efficiency over variable power levels which result from multipath. The powering is performed independent of signal transmission, which differentiates it from RFID tags.

A directly integrated antenna and rectifier with no intermediate matching network, or rectenna, is used to receive and rectify power. Many rectennas are fabricated on microwave substrates, which are costly and are typically not flexible. Most high-volume RFID tags use lightweight flexible paper or plastic substrates in industrial printing processes with coplanar microwave passive circuits fabricated by conductive printing [7].

In this paper, we present a design and implementation method for a low-mass flexible printed rectenna, with efficiency maximized by time-domain waveform shaping of current and voltage across the rectifying element. An example of a 900-MHz single-Schottky diode rectenna with a mass of 2.1 grams is demonstrated to achieve an RF-DC conversion efficiency of 48.6% at only 8 μW/cm^2 incident power density on a constant DC load of 1-kΩ, which were given as design constraints [12]. The design schematic and a photograph of the implementation can be seen in Fig. 1(a) and (b), respectively.

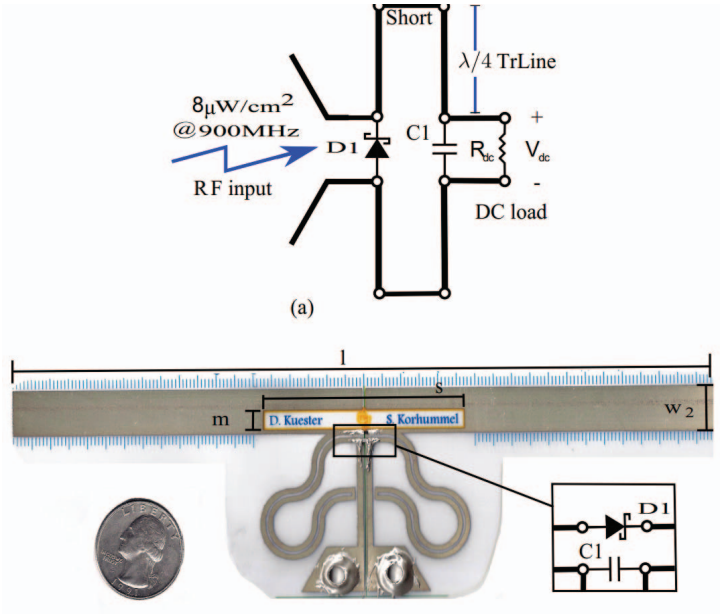

Fig. 1. (a) Circuit diagram of rectenna with shorted quarter-wavelength CPS stub which is an open circuit at the feed-line at f_0 and odd harmonics, and a short at even harmonics due to the capacitor. (b) Photograph of rectenna implemented on a flexible substrate, showing relevant dimensions, diode and capacitor placement; with l=155 mm, m=4.8 mm, s=54.7 mm, w2=10.8 mm

II. Design Procedure

The overall rectenna size is reduced by directly matching a complex antenna impedance to the nonlinear diode impedance at the design frequency for optimum efficiency at a given incident power level. This eliminates the 50-Ω matching circuits, thus reducing the insertion loss, cost, and complexity of the rectenna. The impedance of the diode with respect to the incident RF power,frequency, and the value of the DC load needs to be characterized before antenna design can be accomplished. Once the diode impedance is characterized, the antenna complex impedance needs to be matched to the diode for efficient RF-DC power transfer. The efficiency of rectifiers can be further improved by specific terminations at the harmonics of the operating frequency.

In previous designs, harmonic re-radiation was rejected by

978-1-4673-5010-5/13/$31.00 ©2013 IEEE

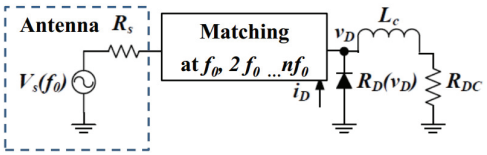

Fig. 2. General microwave rectenna circuit where the antenna is represented as an equivalent source, and includes DC blocking. The matching network includes harmonic terminations, and L_c is an RF choke which isolates the DC load.

terminating the harmonics generated by the diode nonlinearity in shorts or opens [9], [10], which also improves efficiency. Recent work has investigated microwave rectifier design by analogy to amplifier design [8] by wave-shaping of the current and voltage across the nonlinear device, demonstrating a RF-to-DC conversion efficiency of 77.6% for a single harmonically terminated diode. With this in mind, a general rectenna design circuit as illustrated in Fig. 2 is used as a starting design point. A Schottky diode is used as the non-linear element for rectification, and the antenna is modeled as a generator at the fundamental frequency, though we later consider its complex impedance over a wider bandwidth.

A. Class-F Rectifier Analysis and Design

Consider the rectifier circuit shown in Fig. 2 and assume that all even harmonics are terminated in short circuits, while all odd harmonics are terminated in open circuits. This set of harmonic terminations is the same as for a Class-F amplifier. The voltage and current waveforms across the rectifying element can now be derived given the assumed set of harmonic terminations. The fundamental frequency component of the voltage across the diode is given by

$$V_D(f_0) = V_s(f_0) \tag{1}$$

During the second half of the RF cycle, the voltage across the rectifying element must be zero, assuming an ideal rectifier, for which $R_d = 0$ but is in reality a non-ideal on-resistance. This condition must be met through the addition of DC and strictly odd harmonic voltage components, given the enforced harmonic terminations. Therefore, the voltage waveform is expressed as

$$v_D(\theta) = \begin{cases} 2V_{DC}, & 0 \le \theta < \pi \\ 0, & \pi \le \theta < 2\pi \end{cases} \tag{2}$$

A Fourier expansion of (2) expresses the DC component of the voltage waveform as

$$V_{DC} = \frac{\pi}{4} V_D(f_0) \tag{3}$$

The current waveform is then expressed as

$$i_D(\theta) = \begin{cases} 0, & 0 \le \theta < \pi \\ -2I_D(f_0)\sin\theta, & \pi \le \theta < 2\pi \end{cases} \tag{4}$$

A Fourier expansion of (4) expresses the DC component of the current waveform as

$$I_{DC} = \frac{2I_D(f_0)}{\pi} \tag{5}$$

The ideal voltage waveform is a square wave for all harmonics terminated appropriately, and the current is a half-sine wave.

The DC load value can be derived for the optimal rectifier waveforms as:

$$R_{DC} = \frac{\pi^2 V_D(f_0)}{8 I_D(f_0)} = \frac{\pi^2}{8} R_D(f_0) \tag{6}$$

The efficiency of the rectifier may now be determined as the ratio of the DC power dissipated in the load resistance to the available fundamental frequency power:

$$\eta = \frac{P_D C}{P(f_0)} = 2\frac{V_{DC} I_{DC}}{V_D(f_0) I_D(f_0)} = 2\frac{\frac{\pi}{4} V_D(f_0) \frac{2}{\pi} I_D(f_0)}{V_D(f_0) I_D(f_0)} = 1 \tag{7}$$

Therefore, the ideal class-F half-wave rectifier converts all available RF power to DC power if the DC loading resistance set to the value given in (6). The RF-DC conversion efficiency as a function of $R_{DC}/R_s(f_0)$ was simulated in Microwave Office® for varying rectifier on-resistance and the optimal DC load appears to increase as the on-resistance increases. For zero on-resistance, the optimal DC load is exactly that predicted by (6). The reason for the increase in optimal DC load as the on-resistance increases is that by increasing the DC resistance, the current through the on-resistance is reduced, thus reducing the loss. However, there is a penalty paid in reflected power from the rectifying element due to the non-ideal match. This limits the benefit of increasing the DC load infinitely with a fixed fundamental frequency match.

The above Fourier-based approach can be extended to include the on-resistance of the rectifier element and the threshold voltage. The resulting voltage waveform is not an ideal rectangular wave. A Fourier decomposition of the voltage waveform using the transition points must be performed in order to determine the DC and fundamental components of the voltage and current. Thus, the input power can be obtained and the maximal current expressed in terms of the rectifying element parameters, V_{DC} and I_{DC}, $V(f_0)$ and $I(f_0)$ may be calculated, and from these the DC load, fundamental load, and rectifier efficiency are determined. The DC load is given by

$$R_{DC} = \frac{V_{DC}}{I_{DC}} \tag{8}$$

while the load at the fundamental frequency is given by

$$R(f_0) = -\frac{V(f_0)}{I(f_0)} \tag{9}$$

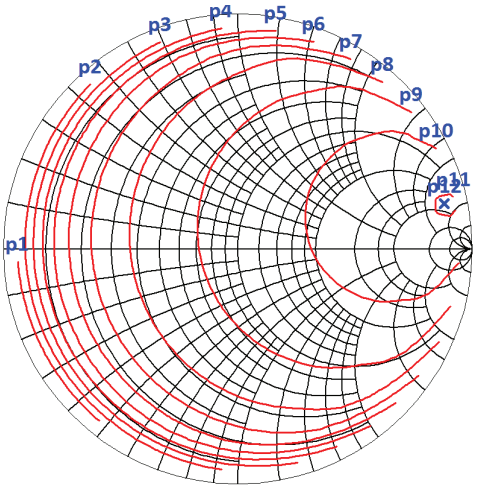

Fig. 3. Simulated load-pull constant power contour curves for 0 dB RF power has -1.5413 dB DC power out at the optimum impedance of 181+j375Ω with Class-F harmonic terminations.

The negative impedance in (9) indicates that power is delivered to the rectifying element rather than created by the rectifying element.

Based on the theory above, AWR Microwave Office simulations were used to characterize the impedance of the Skyworks Schottky diode from the Modelithics Library v8.0 using load-pull simulations, first with no harmonics terminated, then with class F terminations. It is shown that that with all other rectification parameters being the same, (e.g. DC load, frequency, RF input power, and component values) the class F terminations increase the RF-DC conversion by 8%. Simulations resulted in an optimal impedance of Z_d=252-j410Ω for no harmonic terminations and Z_d=181-j375Ω, with class F terminations. The impedances, or in this case, reflection coefficients at the second and third harmonic are fixed with a harmonic balance tuner element at $f_0 = 900$ MHz.

The efficiency from the diode SPICE model in the Microwave Office simulation, with ideal harmonic terminations, gives an estimated RF-to-DC conversion efficiency across a 1-kΩ of 70.6%. This gives a target antenna impedance, as seen by the diode, to be on the order of $181 + j375\,\Omega$, the same as the simulated result.

B. Antenna Complex Impedance

In the design procedure for a directly integrated rectifier and antenna, $|S_{11}|$ of the antenna is not the only relevant parameter. The full complex impedance of the antenna needs to be understood at the operating frequency and harmonics. Maximum power transfer to the diode occurs only when the antenna and diode are conjugately matched.

The rectenna was designed with several optimization goals in mind: minimized overall physical dimensions and mass; highest conversion efficiency and a single 1-kΩ DC load value. The compact meandered feed lines are integrated with the coplanar dipole antenna to present the correct harmonic terminations with a gap at the top to block DC and a capacitor

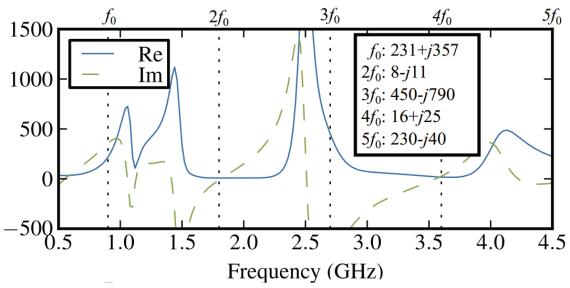

(a)

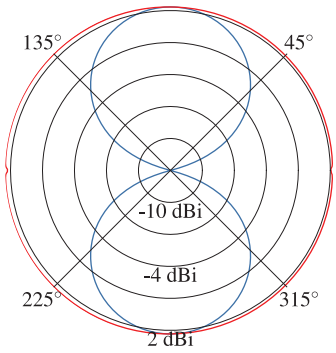

(b)

Fig. 4. Dipole (a) antenna impedance vs. frequency and (b) 900 MHz gain pattern of the E and H fields, simulated in AWR Axiem as well as Ansoft's HFSS.

to short the even harmonics. Adjusting the inset rectangle dimensions s and m varies $Z(f_0)$ across a broad range of inductive values. In order to archive the inductive values needed with the antenna the approach of [11] is to set l, s, m, w_2 for the target Z at the carrier.

III. Implementation and Measurements

The realized rectenna is pictured in Fig. 1(a), with a banana jack to connect the 1 kΩ DC load. The flexible substrate is 0.13 mm-thick polyethylene terephthalate (PET) with relative permittivity $\epsilon_r \approx 3$. A commercial inkjet prints Methode 9101 conductive silver ink traces, with a nominal bulk conductivity of 15 MS/m and 2 µm thickness. We measured 60 mΩ/□ sheet resistance of at DC, which were used in full-wave simulation. The chips are bonded to the substrate with silver epoxy. Simulated complex impedance of this antenna design is shown in Fig. 4. At $2f_0$ and $4f_0$, $|Z|$ is more than seven times smaller than at the fundamental. At $3f_0$, the highly capacitive $|Z|$ appears highly reflective, thanks to the sharp resonance nearby.

Measurements were performed in an anechoic chamber with a calibrated sweeper and broad-band calibrated horn antenna. From these measurements, the efficiency (conversion loss) can be estimated, assuming the simulated antenna gain stays the same when integrated with a rectifier. The conversion loss as a function of DC load resistance and the efficiency as a function of incident plane wave power density are shown in Fig. 5. The optimal operating point P_{RF}=8 μW/cm^2 corresponds to

Antenna gain, G	2.3 dBi
Input impedance, Z	231+j357 Ω

(a) Simulated printed structure parameters

DC power output, P_{dc}	0 dBm
Est. DC/RF conversion efficiency	50%
Optimal DC load, R_{dc}	1 kΩ

(b) Measured performance
(P_{RF}=8 μW/cm^2, $R_{dc} = 1\,\text{k}\Omega$)

Dimensions	$155 \times 46 \times 0.13\,\text{mm}^3$
Mass	2.1 g

(c) Physical parameters

TABLE I
RECTENNA CHARACTERISTICS AT 900 MHZ

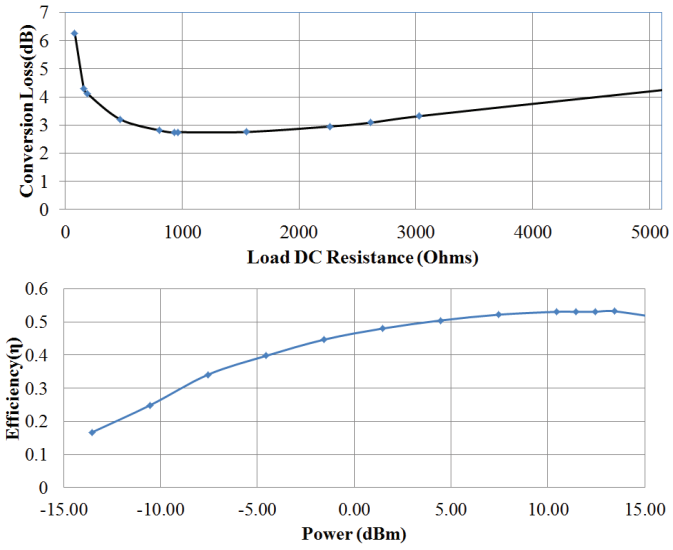

Fig. 5. RF-DC conversion loss measured at 900 MHz as a function of DC load resistance with fixed P_{RF}=8 μW/cm^2 (a) and efficiency as a function of incident power $\mathcal{P}$ with fixed $R_{dc} = 1\,\text{k}\Omega$, given by specifications in [12].

slightly less than 1 mW power input and 0.5 mW output. Final performance data are summarized in Table I.

IV. CONCLUSION

This design demonstrates that at least half of available RF power can be rectified to DC on a low-cost flexible substrate with a class-F rectifier, with very low incident power density. The goal was to use direct integration to eliminate loss due to a matching circuit, enabling use of inexpensive lossy printed substrates. Although the results are improved compared to a constant-impedance RF feed, there is still more loss than in bulkier designs in, e.g. [9], [10] which use standard substrates with relatively thick metal. We are investigating whether the conversion loss can be reduced further with this diode and fabrication process. Some possible sources for the discrepancies include poor fabrication repeatability and unanticipated interactions between the DC test lines and the rectenna. The half-wavelength transmission line structure makes this practical primarily when the power harvesting antenna is larger than roughly $\lambda/4$. This approach is therefore most practical at shorter wavelengths (e.g. higher-frequency bands near 2.4 and 5.8 GHz). This feed's modest efficiency improvement may apply directly to RFID. The improved power harvesting, and therefore chip sensitivity, may extend the turn-on range of RFID tags without any modification to existing chips.

ACKNOWLEDGMENT

The authors are grateful to Dr. M. Roberg, now with Triquint Semiconductor, for his advice on class-F rectification, and the NIST antenna lab for use of its conductive ink printer and standard gain antennas. This work was supported by the Hudson Moore Jr. professorship at the University of Colorado at Boulder.

REFERENCES

[1] Falkenstein, E.; Costinett, D.; Zane, R.; Popovic, Z.; , "Far-Field RF-Powered Variable Duty Cycle Wireless Sensor Platform,"in *Circuits and Systems II: Express Briefs, IEEE Transactions on* , vol.58, no.12, pp.822-826, Dec. 2011

[2] Hagerty, Joseph A.; Lopez, Nestor D.; Popovic, Branko; Popovic, Zoya; , "Broadband Rectenna Arrays for Randomly Polarized Incident Waves *Microwave Conference, 2000. 30th European , vol., no., pp.1-4, Oct. 2000*

[3] E. Falkenstein, M. Roberg, and Z. Popović, "Low-Power Wireless Power Delivery," *IEEE Transactions Microwave Theory Techniques*, vol. 60, no. 7, pp. 2277–2286, 2012

[4] Bernhard, J.T.; Hietpas, K.; George, E.; Kuchima, D.; Reis, H.; , "An interdisciplinary effort to develop a wireless embedded sensor system to monitor and assess corrosion in the tendons of prestressed concrete girders," in *Wireless Communication Technology, 2003. IEEE Topical Conference on* , vol., no., pp. 241- 243, 15-17 Oct. 2003

[5] Vyas, Rushi; Nishimoto, Hiroshi; Tentzeris, Manos; Kawahara, Yoshihiro; Asami, Tohru; , "A battery-less, energy harvesting device for long range scavenging of wireless power from terrestrial TV broadcasts,' ' *Microwave Symposium Digest (MTT), 2012 IEEE MTT-S International* , vol., no., pp.1-3, 17-22 June 2012

[6] Collado, Ana; Georgiadis, Apostolos; , "Improving wireless power transmission efficiency using chaotic waveforms," *Microwave Symposium Digest (MTT), 2012 IEEE MTT-S International* , vol., no., pp.1-3, 17-22 June 2012

[7] L. Yang, A. Rida, R. Vyas, and M. M. Tentzeris, "RFID tag and RF structures on a paper substrate using inkjet-printing technology," *Microwave Theory and Techniques, IEEE Transaction*, vol. 55, no. 12, pp. 2894–2901, 2007.

[8] Roberg, M.; Reveyrand, T.; Ramos, I.; Falkenstein, E. A.; Popovic, Z.; ,"High-Efficiency Harmonically Terminated Diode and Transistor Rectifiers *Microwave Theory and Techniques, IEEE Transactions on , vol.60, no.12, pp.4043-4052, Dec. 2012*

[9] J. Park, S.-M. Han, and T. Itoh, "A rectenna design with harmonic-rejecting circular-sector antenna," *IEEE Ant. Wireless Prop. Letters*, vol. 3, pp. 52–54, 2004.

[10] H. Takhedmit, L. Cirio, B. Merabet, B. Allard, F. Costa, C. Vollaire, and O. Picon, "Efficient 2.45 GHz rectenna design including harmonic rejecting rectifier device," *Electronics Letters*, vol. 46, no. 12, p. 811, 2010.

[11] N. Mohammed, K. Demarest, and D. Deavours, "Analysis and synthesis of UHF RFID antennas using the embedded T-match," in *2010 IEEE Intl. Conf. RFID*. IEEE, 2010, pp. 230–236.

[12] http://ims2012.mtt.org/files/SDC4_Final.pdf